International Journal of Power Electronics and Drive System (IJPEDS)
Vol. 17, No. 4, December 2026, pp. 2486~2494
ISSN: 2088-8694, DOI: 10.11591/ijpeds.v17.i4.pp2486-2494

Study on adaptive control of solar panel array systems based on the changing direction of the sun throughout the day

Tran Duc Chuyen, Doan Van Vu
Faculty of Electrical Engineering – Automation, University of Economics - Technology for Industries, Hanoi, Vietnam

Article Info

Article history:

Received Aug 12, 2026
Revised Sep 18, 2026
Accepted Oct 4, 2026

Keywords:

Adaptive control
Intelligent control
PMSM engine
Position control
Solar energy
Solar panel controller

ABSTRACT

This paper presents the research, calculations, and design of an automatic electric drive control system for a solar panel array (ACDSPA) with a permanent magnet synchronous motor (PMSM) using an adaptive control method that takes into account disturbances. Here, the optimal adaptive controller is designed to demonstrate greater convergence than conventional control. Based on the adaptive law developed, control parameters, especially self-tuning parameters during the control process, are updated quickly online. Therefore, disturbances and nonlinearity can be better reduced for the intelligent electric drive system (IEDS). A reference model based on Lyapunov theory is then created to track angular position errors. The adaptive law control system with model reference proposed by the authors in this paper combines the advantages of adaptive model-based control methods to control this IEDS system. Simulation results show faster performance and more accurate control compared to other control methods. This also provides a basis for future research, design, fabrication, and algorithm development of an intelligent controller AI for the ACDSPA auto-tracking system and renewable energy battery systems in the future.

This is an open access article under the CC BY-SA license.

Corresponding Author:

Tran Duc Chuyen
Faculty of Electrical Engineering – Automation, University of Economics - Technology for Industries
Hanoi, Vietnam
Email: tdchuyen@uneti.edu.vn

1. INTRODUCTION

Currently, the automation process of some intelligent electric drive systems (IEDS) of industrial machinery is developing strongly. In Figure 1, the automatic control drive system for solar panel arrays (ACDSPA) always needs to work with high accuracy and limited rotation angle [1]-[5]. These are the precision drive systems of computer numerical control (CNC) metal cutting machines, lathes, drills, milling machines, planers, and ACDSPA systems. Therefore, this paper uses speed control and position control of permanent magnet synchronous motor (PMSM) motors for ACDSPA to control solar panel arrays using adaptive control algorithms to improve the control quality of the system [6]-[9]. On that basis, by measuring and calculating, estimating the current and voltage components of the motor's rotation angle and speed to evaluate the output components [10]-[13]. From there, we study the design, calculation, and simulation modeling of the drive system based on adaptive control methods using PMSM motors, taking into account noise factors, in the synthesis of the controller [14]-[17]. Then, in order to improve the control accuracy of ACDSPA IEDS to bring out the maximum power obtained by the solar power system [18]-[22].

With some recent studies on the problem of speed and position control for rotating electrical machines, in order to achieve the speed value and accurate position response, speed, and position sensors are used [5], [10] this research has not brought high efficiency to the automatic control system. Some authors have used classical (old) controllers for calculation and traditional (inefficient) controllers with low control quality,

such as using proportional-integral-derivative to calculate estimates, fuzzy sliding mode, PD method combined with adaptive sliding mode control (ASMC), proportional–integral (PI) controller combined with sliding mode control, adaptive control combined with neural networks, and adaptive controllers in industrial drive systems [3], [4]. For second- and third-order linear controllers – linear quadratic regulator (LQR) and many other classical controllers, the authors have recently also used direct measurement methods to calculate controller parameters [8], [10], [13]. In document [7], adaptive control programming for the system is studied, and in [14] an economic-technical analysis is given between fixed solar panels and solar panels capable of tracking the sun's direction. In [18], a design and simulation of a photovoltaic solar energy tracking system based on mechanical coordinates is conducted, without using adaptive algorithms for control. In [23], a filtered sun sensor for solar tracking in PV panels and systems is studied, without studying the automatic adaptive tracking of sunlight. Recently, these methods have not yet improved the control quality for IEDS for ACDSPA in the direction of the sun's change during the day, which is currently needed [17], [21], [24]. Therefore, to ensure ACDSPA operates accurately and safely, improves the quality of control, and reduces product costs, it is necessary to consider saving electricity to reduce costs [25]. The system needs to be accurate and always ensure that ACDSPA adheres to the set value so that the solar panel array always absorbs the light into the panels; then the amount of electricity collected will reach the maximum [6], [26], [27].

Figure 1 shows the ACDSPA structure using a PMSM motor based on adaptive control. The electrical part includes a power supply, a power electronic converter, a control system to generate control laws, and the PMSM motor; the mechanical part includes a speed reducer (flexible coupling) connected to the working mechanism. Here, the control system used has a clear control model and control method. Therefore, in this paper, the authors use adaptive control methods to design, calculate parameter estimates, and establish algorithms, with the PMSM motor as the control object for ACDSPA. This is a new step in addressing a problem that is currently attracting research interest from scientists both domestically and internationally.

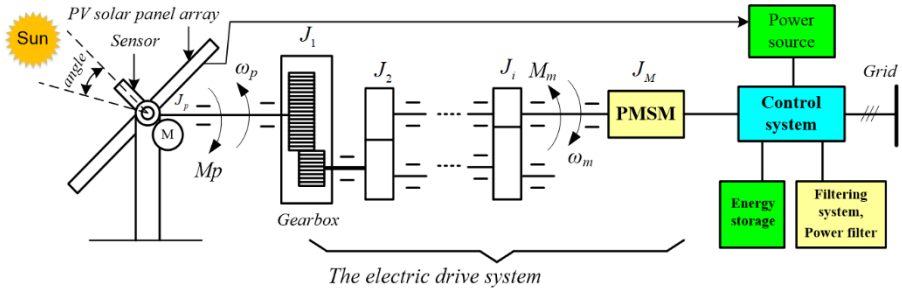

Figure 1. The block diagram of the ACDSPA structure using PMSM

2. STUDY OF ADAPTIVE CONTROL MODELS AND ALGORITHMS FOR ACDSP

2.1. Developing a PMSM motor control model for ACDSPA

From the IEDS model with the structure introduced in Figure 1, the author proceeded to study the PMSM motor with its spatial vector coordinates as shown in Figure 2 [2], [5]. Next, we obtain the spatial vector coordinates with the dq system as the reference coordinate system, from which the mathematical model of the PMSM motor is represented as (1) to (3).

$$\frac{di_d}{dt} = \frac{1}{L_q}\left[-R_s i_d + pL_q i_q \varphi_r + v_d\right] \quad (1)$$

$$\frac{di_q}{dt} = \frac{1}{L_q}\left[-R_s i_q - pL_d i_d \varphi_r - p\sqrt{\frac{3}{2}}\psi_{sF}\varphi_r + v_q\right] \quad (2)$$

$$\frac{d\varphi_r}{dt} = \frac{1}{I}\left[p\sqrt{\frac{3}{2}}\,\psi_{sF} i_q + p(L_d - L_q) i_d i_q - F\varphi_r - D_r\right] \quad (3)$$

In (1), we explain that the components $v_d(t), v_q(t)$ are the stator voltage values of the d-axis and q-axis, respectively; the current components $i_d(t), i_q(t)$ d are the stator currents of the d-axis and q-axis, respectively; L_s is the stator inductance; R_s is the stator resistance value; $\varphi_r(t)$ is the angular velocity of the motor rotor; I is the system moment of inertia; ψ_{sF} is is the magnetic flux linkage of the motor rotor; D_r is

the load torque component; p is the number of pole pairs; F is the viscous friction coefficient. From (1) to (3), the state-space model of the PMSM motor is represented as (4) to (6).

$$\dot{x}_1 = \frac{1}{L_d}\left[-R_s x_1 + pL_q x_2 x_3 + \varepsilon_1\right] \tag{4}$$

$$\dot{x}_2 = \frac{1}{L_q}\left[-R_s x_2 - pL_d x_1 x_2 - p\sqrt{\frac{3}{2}}\psi_{sF} x_3 + \varepsilon_2\right] \tag{5}$$

$$\dot{x}_3 = \frac{1}{I}\left[p\sqrt{\frac{3}{2}}\psi_{sF} x_2 + p\left(L_d - L_q\right)x_1 x_2 - F x_3 - D_r\right] \tag{6}$$

There, $x_1 = i_d, x_2 = i_q, x_3 = \varphi_r, \varepsilon_1 = v_d, v$ and $\varepsilon_2 = v_q$. Variables ε_1 and ε_2 is the actual control and x is the state vector.

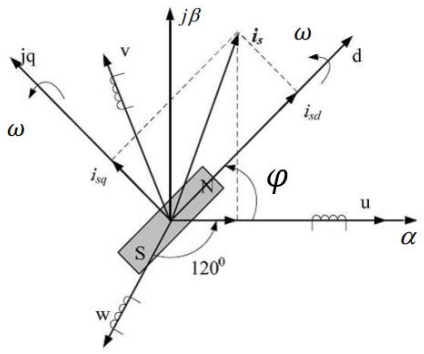

Figure 2. Coordinate system model in space of the PMSM motor

2.2. Research on adaptive motor control algorithms for PMSM for ACDSPA

The steps for constructing the control law based on state feedback control theory and related Lyapunov functions for the ACDSPA system are as follows. Here, we consider the PMSM object with high-precision operation in the control with a component where $(L_d \neq L_q)$. Therefore, the actual variable x_1 is forced to zero. To achieve this, an error ϑ_1 is written (7).

$$\vartheta_1 = x_1 - x_1^*; \text{ with } x_1^* = 0 \tag{7}$$

With the reference current of axis x_1^*. Then, taking the derivative of ϑ_1 we have (8).

$$\dot{\vartheta}_1 = \dot{x}_1 - 0 = \frac{1}{L_d}\left[-R_s x_1 + pL_q x_2 x_3 + \varepsilon_1\right] \tag{8}$$

Let's consider the Lyapunov function chosen as (9).

$$V_1 = \frac{1}{2}\vartheta_1^2 > 0 \tag{9}$$

Then, the time derivative of the Lyapunov function is (10).

$$\dot{V}_1 = \vartheta_1\dot{\vartheta}_2 = \frac{\vartheta_1}{L_d}\left(-R_s x_1 + pL_q x_2 x_3 + \varepsilon_1\right) \tag{10}$$

Now we choose $\dot{\vartheta}_1$ as (11).

$$\dot{\vartheta}_1 = -\Delta_1\vartheta_1 \text{ với } \Delta_1 > 0 \tag{11}$$

Then, such that Δ_1 is a design parameter, we have (12).

$$\dot{V}_1 = \dot{\vartheta}_1\vartheta_1 = -\Delta_1\vartheta_1^2 < 0 \tag{12}$$

This problem shows that the error ϑ_1 is varying exponentially $\vartheta_1 \to 0$. Therefore, the equilibrium point ($\vartheta_1 = 0$) is globally asymptotically stable (GAS), [3], [4], [10]. From there, consider the control law of the d-axis current generated by combining (8) and (11) as (13).

$$\varepsilon_1 = -L_d \Delta_1 \varepsilon_1 + R_s x_1 - p L_q x_2 x_3 \tag{13}$$

Then we proceed with the tracking error ϑ_2 which is written (14).

$$\vartheta_2 = x_3 - v_{\mathrm{d}}^* \tag{14}$$

With, v_{d}^* speed set. From (14), we deduce from (6) to obtain (15).

$$\dot{\vartheta}_2 = \dot{x}_3 - v_{\mathrm{d}}^* = \frac{1}{I}\left[p\left(\psi + L_{dq} x_1\right) x_2 - F x_3 - D_r\right] - \dot{v}_{\mathrm{d}}^* \tag{15}$$

In which, $v_{\mathrm{d}}^* = \omega_{ref}^*; L_{dq} = \left(L_d - L_q\right); \psi = \sqrt{\frac{3}{2}}\psi_{sF}$. In (15), the quantity x_2 acts as the virtual control variable. To determine the trajectory of this virtual control variable, the following second Lyapunov function is considered as (16).

$$V_2 = \frac{1}{2}\vartheta_2^2 > 0 \tag{16}$$

Differentiating with respect to time, we have (17).

$$\dot{V}_2 = \vartheta_2 \left[\frac{1}{I}\left[p\left(\psi + L_{dq} x_1\right) x_2 - F x_3 - D_r\right] - \dot{v}_{\mathrm{d}}^*\right] \tag{17}$$

The (17) shows that the tracking error ϑ_2 can be adjusted to 0 if the ACDSPA dynamics are chosen as (18).

$$\dot{\vartheta}_2 = -\Delta_2 \vartheta_2 \tag{18}$$

There, $\Delta_2 > 0$ is the design parameter. Combining (15) and (18), the following stability function is determined by (19).

$$p\left(L_{dq} x_1 + \psi\right) x_2 = I(\dot{v}_{\mathrm{d}}^* - \Delta_2 \vartheta_2) + F x_3 + D_r \tag{19}$$

In which, $p\left(L_{dq} x_1 + \psi\right) x_2$ is the virtual control input variable. Since $p\left(L_{dq} x_1 + \psi\right) x_2$ is not a control input that yields an effective value, according to the stability theory in documents [3], [4], [11], we have (20):

$$\beta = I(\dot{v}_{\mathrm{d}}^* - \Delta_2 \vartheta_2) + F x_3 + D_r \tag{20}$$

This stability problem acts as a reference q-axis current. On the other hand, the parameters I and F are not measurable, and the damping torque D_r depends on the load change or the trajectory of the solar array, which are unknown. These parameters will be estimated by an adaptive control method, which enhances the sustainability and stability of the system: Then, taking the derivative of the Lyapunov function (18) takes the form (19) as (21).

$$\beta = \hat{I}(\dot{v}_{\mathrm{d}}^* - \Delta_2 \vartheta_2) + \hat{F} x_3 + \hat{D}_r \tag{21}$$

In this case, $\hat{I}$, $\hat{F}$, and $\hat{D}_r$ are the estimated values of I, F, and D_r respectively. We keep the expression for β unchanged and introduce a new error. Therefore, the error ϑ_3 is defined as (22).

$$\vartheta_3 = \beta - p\left(L_{dq} x_1 + \psi\right) x_2 \tag{22}$$

Then we notice that in the steady state, x_1 tends to be zero. Next, we establish the law of variation of the control signal ϑ_2: Using (21) and (22), (15) becomes (23).

$$\dot{\vartheta}_2 = -\Delta_2\vartheta_2 - \frac{\tilde{I}}{I}(\dot{v}_{\mathrm{d}}^* - \Delta_2\vartheta_2) - \frac{\tilde{F}}{I}x_3 - \frac{\tilde{D}_r}{I} - \frac{\vartheta_3}{I} \tag{23}$$

In which, $\tilde{I},\ \tilde{F}$, and $\tilde{D}_r$ are the errors of I, F và D_r and, $\tilde{I} = I - \hat{I};\ \tilde{F} = F - \hat{F};\ \tilde{D}_r = D_r - D_r$. Then (17) of the Lyapunov function is rewritten as (24).

$$\dot{V}_2 = -\Delta_2\vartheta_2^2 - \left[\frac{\tilde{I}}{I}(\dot{v}_{\mathrm{d}}^* - \Delta_2\vartheta_2) + \frac{\tilde{F}}{I}x_3 + \frac{\tilde{D}_r}{I} - \frac{\vartheta_3}{I}\right]\vartheta_2 \tag{24}$$

From (23), the time derivative of $\dot{\vartheta}_3$, using (5), (1), and (21), we get (25).

$$\dot{\vartheta}_3 = \dot{\hat{I}}(\dot{v}_{\mathrm{d}}^* - \Delta_2\vartheta_2) + \dot{\hat{F}}x_3 + \dot{\hat{D}}_r + \hat{I}\dot{v}_{\mathrm{d}}^* + \hat{F}\ddot{v}_{\mathrm{d}}^* - \left(\hat{F} - \Delta_2\hat{I}\right)[\Delta_2\vartheta_2 + \frac{\tilde{I}}{I}(\dot{v}_{\mathrm{d}}^* - \Delta_2\vartheta_2) + \frac{\tilde{F}}{I}x_3 + \frac{\tilde{D}_r}{I} - \frac{\vartheta_3}{I} + \Delta_1 p x_2 L_{dq}\vartheta_1] - \frac{p}{L_q}\left(L_{dq}x_1 + \psi\right)[-R_s x_2 - pL_d x_1 x_3 - p\psi x_3 + \varepsilon_2] \tag{25}$$

At this point, we can conveniently select the control signal ε_2 to stabilize the entire system with state vectors ϑ_2, ϑ_3. To do this, consider the proposed extended Lyapunov function as (26).

$$V_3 = V_2 + \frac{1}{2}\vartheta_3^2 + \frac{1}{2}\frac{1}{\mu_1}\frac{\tilde{I}^2}{I} + \frac{1}{2}\frac{1}{\mu_2}\frac{\tilde{D}_r^2}{I} + \frac{1}{2}\frac{1}{\mu_3}\frac{\tilde{F}^2}{I} > 0 \tag{26}$$

Where, μ_1, μ_2, μ_3 are the controller parameters, respectively. Differentiating with respect to time (27).

$$\dot{V}_3 = \dot{V}_2 + \dot{\vartheta}_2\vartheta_3 + \frac{\dot{\tilde{I}}}{\mu_1}\frac{\tilde{I}}{I} + \frac{\dot{\tilde{D}}_r}{\mu_2}\frac{\tilde{D}_r}{I} + \frac{\dot{\tilde{F}}}{\mu_3}\frac{\tilde{F}}{I} \tag{27}$$

Using (24) and (25), expression (26) becomes (28):

$$\dot{V}_3 = -\Delta_2\vartheta_2^2 - \Delta_3\vartheta_3^2 + \frac{\tilde{I}}{I}\left[\frac{\dot{\tilde{I}}}{\mu_1} + (\Delta_2\vartheta_2 - \dot{v}_{\mathrm{d}}^*)\left(\vartheta_2 + \left(\hat{F} - \Delta_2\hat{I}\right)\right)\vartheta_3\right] + \frac{\tilde{D}_r}{I}\left[\frac{\dot{\tilde{D}}_r}{\mu_2} - \left(\vartheta_2 + \left(\hat{F} - \Delta_2\hat{I}\right)\right)\vartheta_3] + \frac{\tilde{F}}{I}[\frac{\dot{\tilde{F}}}{\mu_3} - \left(\vartheta_2 + \left(\hat{F} - \Delta_2\hat{I}\right)\vartheta_3\right)x_3\right] \tag{28}$$

Then we assume that (29).

$$\begin{bmatrix} \dot{\hat{I}}(\dot{v}_{\mathrm{d}}^* - \Delta_2\vartheta_2) + \dot{\hat{F}}x_3 + \dot{\hat{D}}_r + \hat{I}\ddot{v}_{\mathrm{d}}^* - \dot{\hat{F}}\dot{v}_{\mathrm{d}}^* - \frac{\vartheta_2}{I} - \left(\hat{F} - \Delta_2\hat{I}\right)\left(\frac{\vartheta_3}{I} + \Delta_2\vartheta_2\right) \\ +\Delta_1 p x_2 L_{dq}\vartheta_1 - \frac{p}{L_q}\left(L_{dq}x_1 + \psi\right)(-R_s x_2 - pL_d x_1 x_3 - p\psi x_3 + \varepsilon_2) \end{bmatrix} = -\Delta_3\vartheta_3 \tag{29}$$

In which, $\Delta_3 > 0$ is the third design parameter. However, (28) shows that the control signal ε_2 should be chosen so that the terms in the curly braces are set to zero. This helps us propose an adaptive control theory aimed at estimating the three parameters as (30).

$$\dot{\hat{I}} = -\delta_I;\ \dot{\hat{D}}_r = -\delta_{D_r};\ \dot{\hat{F}} = -\delta_F \tag{30}$$

Then we have:

$$\delta_I = (\Delta_2\vartheta_2 - \dot{v}_{\mathrm{d}}^*)\left(\vartheta_2 + \left(\hat{F} - \Delta_2\hat{I}\right)\vartheta_3\right)\mu_1 \tag{31}$$

$$\delta_{D_r} = -\left(\vartheta_2 + \left(\hat{F} - \Delta_2\hat{I}\right)\vartheta_3\right)x_3\mu_2 \tag{32}$$

$$\delta_F = -\left(\vartheta_2 + \left(\hat{F} - \Delta_2\hat{I}\right)\vartheta_3\right)\mu_3 \tag{33}$$

From (23) and (30) to (33), the estimated parameters of the PMSM and the estimated load moment $\hat{D}_r$ are calculated using the updated rule expression, as in (34).

$$\dot{\hat{I}} = \delta_I;\ \dot{\hat{D}}_r = \delta_{D_r};\ \dot{\hat{F}} = \delta_F \tag{34}$$

We have the ACDSPA architecture diagram using a PMSM based on the adaptive control method as shown in Figure 3.

Therefore, using (30) to (34), (28) becomes (35).

$$\dot{V}_3 = -\Delta_2 \vartheta_2^2 - \Delta_3 \vartheta_3^2 < 0 \tag{35}$$

The (35) shows that the equilibrium point $(\vartheta_2, \vartheta_3) = (0, 0)$ is globally asymptotically stable. Therefore, from (35), the control law is given by (36).

$$\varepsilon_2 \frac{L_q}{p(L_{dq}x_1+\psi)}\left[\dot{\hat{I}}\,(v_{\mathrm{d}}^* - \Delta_2\vartheta_2) + \dot{\hat{F}}x_3 + \dot{\hat{D}}_r + \hat{I}\dot{v}_{\mathrm{d}}^* - \hat{F}\dot{v}_{\mathrm{d}}^* - \left(\hat{F} - \Delta_2\hat{I}\right)\left(\frac{\vartheta_3}{I} + \Delta_2\vartheta_2\right) + \Delta_1 p x_2 L_{dq}\vartheta_1 - \right.$$
$$\left.\frac{\vartheta_2}{I} + \frac{p}{L_q}\left(L_{dq}x_1 + \psi\right)R_s x_2 + \Delta_3\vartheta_3 + \frac{p}{L_q}\left(L_{dq}x_1 + \psi\right)\mathrm{p}\left(L_{dq}x_1 + \psi\right)x_3\right] \tag{36}$$

Here, we prove that the following global Lyapunov function is defined by V in (37).

$$V = V_1 + V_2 = \frac{1}{2}\vartheta_2^2 + \frac{1}{2}\vartheta_2^2 + \frac{1}{2}\vartheta_3^2 + \frac{1}{2}\frac{1}{\mu_1}\frac{\tilde{I}^2}{I} + \frac{1}{2}\frac{1}{\mu_2}\frac{\tilde{D}_r^2}{I} + \frac{1}{2}\frac{1}{\mu_3}\frac{\tilde{F}^2}{I} \tag{37}$$

Its time derivative, using (12) and (36), is obtained as (38).

$$\dot{V}_3 = -\Delta_1\vartheta_1^2 - \Delta_2\vartheta_2^2 - \Delta_3\vartheta_3^2 \tag{38}$$

From (37) and (38), we have positive definite V and negative definite $\dot{V}$, which clearly means that at the equilibrium point (ϑ_1, ϑ_2, ϑ_3) = (0, 0, 0), the ACDSPA system is globally asymptotically stable GAS.

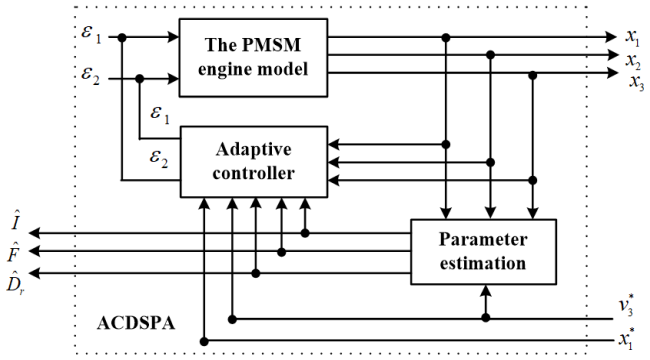

Figure 3. Block diagram of ACDSPA structure using PMSM based on adaptive control

3. RESULTS AND DISCUSSION

After studying the calculations and control algorithm as described above, we proceed to study IEDS for ACDSPA using a PMSM motor with the following parameters: Power 2.0 kW; Rated torque 12.2 Nm; rated torque = 1500 rpm; stator resistance R_{stato} 0.56 Ω; moment of inertia 0.0028 kg.m^2; stator inductance 6.65×10^{-3} H; p = 3; torque constant 2.56 Nm/A; linkage flux ψ_{sF} is 0.82 Wb; viscous friction torque constant 0.0001 Nm /rad.s^{-1}; shaft inductance L_d là 0.048H; shaft inductance q with L_q là 0.064 H. Perform simulations with an adaptive controller for: $\mu_1 = 3.10^{-3}$; $\mu_2 = 5.10^{-3}$; $\mu_3 = 7.10^{-3}$ and $\Delta_1 = 20$; $\Delta_2 = 2.10^{-3}$; $\Delta_3 = 200$, disturbances $D_r = (2.0 \div 5)\,Nm$. From this, we obtain the following simulation results:

Simulation with speed and position responses when changing at both high and low speeds of ACDSPA: at the initial speed of 500 rpm, the blue line (speed 1) is the response speed, and the red line is the set speed. When the speed changes at 2.3 s (I_q changes to 1.5 A) and 4.2s (I_q changes to 1.25 A), from 500 to 600 rpm, the system still operates stably; the output still closely follows the set speed (Figure 4). The current response values I_d (0.02A) and I_q (approximately 0.5 A) accurately reflect the working process, even when changing speed at different times; as the speed changes, the Id and Iq values also change (Figure 5).

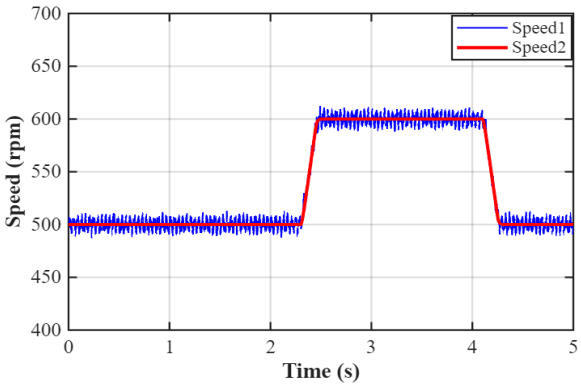

Figure 4. ACDSPA speed characteristics when changing speed

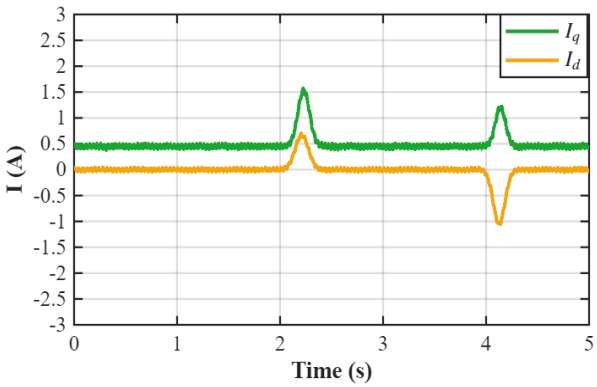

Figure 5. The values of current I_d and I_q when changing the speed of ACDSPA

Figure 6 simulates the system with a low rotational speed of 21 rpm. In this case, the system is connected to the ACDSPA system with a gearbox. With a set speed of n_1 (blue line) and a response speed of n_2 (red line), the system operates stably with negligible oscillations. The output closely tracks the input during stable operation (Figure 6). The simulation results show that when the load torque is estimated at 0.5 Nm at the initial time from 0 to 0.18 s, the system oscillates but can still be estimated and identified according to the set value; the M2 curve "light blue" closely follows the M1 set value "blue curve" Figure 7.

Figure 8 shows the angular control response of the ACDSP when the input angle is small, at 0.1 rad; initially, from 0 to 0.18s, the system oscillates and then remains in equilibrium. The angular tracking error is small, as shown in Figure 9. Simulation with angular position according to a sinusoidal harmonic function (ωt). With a small set angle of 0.5 rad in Figure 10, the set value is the dashed line "1", and the response value is line "2". The response to the disturbance detection torque value with a torque of 0.5 Nm is shown in line M1 as the set value and line M2 as the estimated detection value, as in Figure 11.

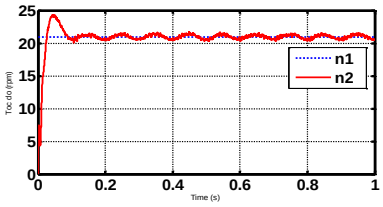

Figure 6. Low rotational speed characteristics of ACDSP

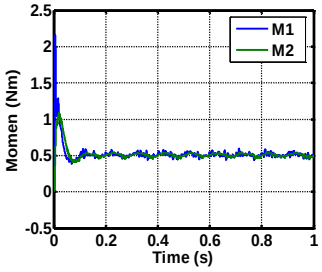

Figure 7. Estimated torque component value as a function of speed

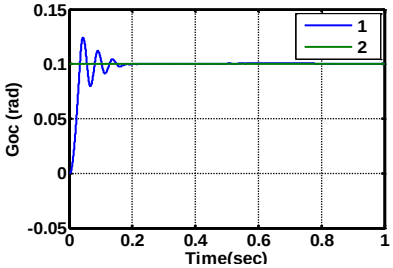

Figure 8. Small angular position value of ACDSP

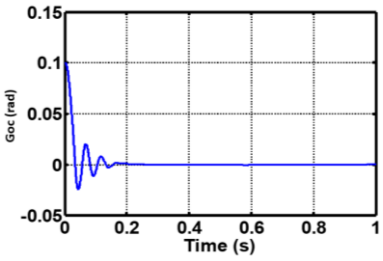

Figure 9. Angular tracking error occurs when the rotation angle of the ACDSP is small

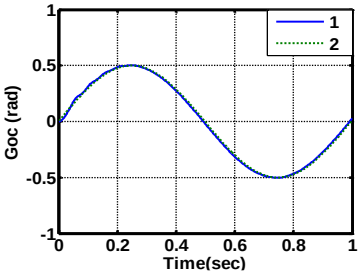

Figure 10. Response to input load according to the harmonic function sin(ωt)

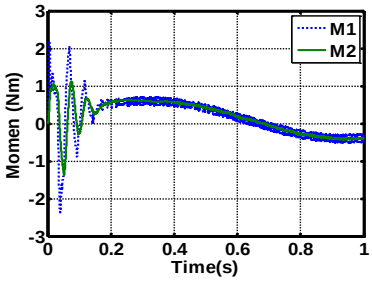

Figure 11. Moment estimator and identifier

4. CONCLUSION

The simulation results of the adaptive algorithm shown above indicate that the working position and angle values of the IEDS controlling the ACDSP always need to respond precisely to changes in torque at different increase and decrease points, while maintaining good system quality. The estimated values of the position-angle and torque calculations of the PMSM motor closely track the input response. This shows that IEDS operates with high quality when controlling the rotor's position and angle, ensuring a high-quality control process for the ACDSP. Compared to other methods such as backstepping, sliding mode control, fuzzy control, neural network control, robust control, or robust adaptive control, the adaptive controller proposed by the authors for ACDSP using PMSM is always considered optimal and achieves high control quality. The proposed adaptive control system's angular control response exhibits stable dynamic characteristics even during transients and acceleration/deceleration, with static error almost completely eliminated in this IEDS. This allows the ACDSP system to maximize energy (power) output, resulting in high economic efficiency. Based on this, the direction for developing newer algorithms combines adaptive optimal control with AI-enhanced learning rules to identify changes in load, nonlinear friction, and elasticity of this drive system.

FUNDING INFORMATION

This research was supported by Faculty of Electrical - Automation; University of Economics and Technology for Industries; No. 353 Tran Hung Dao Road, Ninh Binh Province-Vietnam National; http://www.uneti.edu.vn/.

AUTHOR CONTRIBUTIONS STATEMENT

This journal uses the Contributor Roles Taxonomy (CRediT) to recognize individual author contributions, reduce authorship disputes, and facilitate collaboration.

Name of Author	C	M	So	Va	Fo	I	R	D	O	E	Vi	Su	P	Fu
Tran Duc Chuyen	✓	✓	✓	✓	✓	✓	✓	✓	✓	✓		✓	✓	
Doan Van Vu	✓	✓			✓	✓		✓	✓	✓	✓	✓		✓

C : **C**onceptualization
M : **M**ethodology
So : **So**ftware
Va : **Va**lidation
Fo : **Fo**rmal analysis
I : **I**nvestigation
R : **R**esources
D : **D**ata Curation
O : Writing - **O**riginal Draft
E : Writing - Review & **E**diting
Vi : **Vi**sualization
Su : **Su**pervision
P : **P**roject administration
Fu : **Fu**nding acquisition

CONFLICT OF INTEREST STATEMENT

Authors state no conflict of interest.

DATA AVAILABILITY

Derived data supporting the findings of this study are available from the corresponding author.

REFERENCES

[1] A. Shimada, *Disturbance Observer for Advanced Motion Control with MATLAB/Simulink*. Wiley, 2023, doi: 10.1002/9781394178131.
[2] L. Keviczky, R. Bars, J. Hetthéssy, and C. Bányász, "Control engineering: MATLAB exercises," *Advanced Textbooks in Control and Signal Processing*, pp. 1–275, 2019, doi: 10.1007/978-981-10-8321-1.
[3] J. Connor and S. Laflamme, "Advanced control theory," in *Structural Motion Engineering*, Switzerland: Springer International Publishing, 2014, pp. 545–599, doi: 10.1007/978-3-319-06281-5_10.
[4] J. Pyrhönen, V. Hrabovcová, and R. S. Semken, *Electrical machine drives control: an introduction*. Wiley, 2016, doi: 10.1002/9781119260479.
[5] Z. Xu, T. Zhang, Y. Bao, H. Zhang, and C. Gerada, "A nonlinear extended state observer for rotor position and speed estimation for sensorless ipmsm drives," *IEEE Transactions on Power Electronics*, vol. 35, no. 1, pp. 733–743, Jan. 2020, doi: 10.1109/TPEL.2019.2914119.
[6] T. D. Chuyen, T. Van Tuyen, and N. T. T. Huong, "Development of electric drive system for solar battery system based on artificial intelligence," in *Proceedings - 12th IEEE International Conference on Control, Automation and Information Sciences, ICCAIS 2023*, Jan. 2023, pp. 346–351, doi: 10.1109/ICCAIS59597.2023.10382317.
[7] D. Liu, S. Xue, B. Zhao, B. Luo, and Q. Wei, "Adaptive dynamic programming for control: a survey and recent advances," *IEEE Transactions on Systems, Man, and Cybernetics: Systems*, vol. 51, no. 1, pp. 142–160, 2021, doi: 10.1109/TSMC.2020.3042876.
[8] K. Kumba, P. Upender, P. Buduma, M. Sarkar, S. P. Simon, and V. Gundu, "Solar tracking systems: advancements, challenges, and future directions: a review," *Energy Reports*, vol. 12, pp. 3566–3583, 2024, doi: 10.1016/j.egyr.2024.09.038.

[9] J. Ahmad *et al.*, "Performance analysis and hardware-in-the-loop (HIL) validation of single switch high voltage gain dc-dc converters for MPP tracking in solar PV systems," *IEEE Access*, vol. 9, pp. 48811–48830, 2021, doi: 10.1109/ACCESS.2020.3034310.
[10] O. T. Mahmood, W. Z. Wan Hasan, N. Azis, N. M. H. Norsahperi, H. R. Ramli, and L. I. Ismail, "An adaptive sliding mode controller with free-will arbitrary time convergence for three-phase rectifiers in autonomous agricultural vehicles," *PLOS One*, vol. 20, no. 8, Aug. 2025, doi: 10.1371/journal.pone.0330424.
[11] J. Liu and X. Wang, *Adaptive sliding mode control for mechanical systems*. China, 2011, doi: 10.1007/978-3-642-20907-9_6.
[12] B. K. Hammad, R. H. Fouad, M. S. Ashhab, S. D. Nijmeh, M. Mohsen, and A. Tasmimi, "Adaptive control of solar tracking system," *IET Science, Measurement and Technology*, vol. 8, no. 6, pp. 426–431, 2014, doi: 10.1049/iet-smt.2013.0293.
[13] C. Jamroen, P. Komkum, S. Kohsri, W. Himananto, S. Panupintu, and S. Unkat, "A low-cost dual-axis solar tracking system based on digital logic design: design and implementation," *Sustainable Energy Technologies and Assessments*, vol. 37, 2020, doi: 10.1016/j.seta.2019.100618.
[14] A. E. Gol and M. Ščasný, "Techno-economic analysis of fixed versus sun-tracking solar panels," *International Journal of Renewable Energy Development*, vol. 12, no. 3, pp. 615–626, 2023, doi: 10.14710/ijred.2023.50165.
[15] R. Sadeghi, M. Parenti, S. Memme, M. Fossa, and S. Morchio, "A review and comparative analysis of solar tracking systems," *Energies*, vol. 18, no. 10, 2025, doi: 10.3390/en18102553.
[16] M. S. Ramli, "Dual-axis solar energy tracking and monitoring system with Arduino as a microcontroller," *Scientific Research Journal*, vol. 20, no. 2, pp. 131–145, 2023, doi: 10.24191/srj.v20i2.22365.
[17] M. C. Ozturk, B. Dogan, and M. K. Yesilyurt, "Energy, exergy, sustainability, and economic analyses of a grid-connected solar power plant consisting of bifacial PV modules with solar tracking system on a single axis," *Science and Technology for Energy Transition (STET)*, vol. 78, 2023, doi: 10.2516/stet/2023015.
[18] S. Rustemli, Z. İlcihan, G. Sahin, and W. G. J. H. M. van Sark, "A novel design and simulation of a mechanical coordinate based photovoltaic solar tracking system," *AIMS Energy*, vol. 11, no. 5, pp. 753–773, 2023, doi: 10.3934/energy.2023037.
[19] A. Musa, E. Alozie, S. A. Suleiman, J. A. Ojo, and A. L. Imoize, "A review of time-based solar photovoltaic tracking systems," *Information (Switzerland)*, vol. 14, no. 4, 2023, doi: 10.3390/info14040211.
[20] A. S. C. Roong and S. H. Chong, "Laboratory-scale single axis solar tracking system: design and implementation," *International Journal of Power Electronics and Drive Systems*, vol. 7, no. 1, pp. 254–264, 2016, doi: 10.11591/ijpeds.v7.i1.pp254-264.
[21] M. Ghassoul, "Single axis automatic tracking system based on pilot scheme to control the solar panel to optimize solar energy extraction," *Energy Reports*, vol. 4, pp. 520–527, Nov. 2018, doi: 10.1016/j.egyr.2018.07.001.
[22] P. V. Gharat, S. S. Bhalekar, V. H. Dalvi, S. V. Panse, S. P. Deshmukh, and J. B. Joshi, "Chronological development of nnovations in reflector systems of parabolic trough solar collector (PTC) - a review," *Renewable and Sustainable Energy Reviews*, vol. 145, Jul. 2021, doi: 10.1016/j.rser.2021.111002.
[23] A. Diaz, R. Garrido, and J. J. Soto-Bernal, "A filtered sun sensor for solar tracking in HCPV and CSP systems," *IEEE Sensors Journal*, vol. 19, no. 3, pp. 917–925, 2019, doi: 10.1109/JSEN.2018.2879460.
[24] O. Bamisile *et al.*, "A brief review and comparative evaluation of nanofluid application in solar parabolic trough and flat plate collectors," *Energy Reports*, vol. 8, no. Supplement 13, pp. 156–166, Nov. 2022, doi: 10.1016/j.egyr.2022.08.078.
[25] L. Salgado-Conrado, "A review on sun position sensors used in solar applications," *Renewable and Sustainable Energy Reviews*, vol. 82, pp. 2128–2146, 2018, doi: 10.1016/j.rser.2017.08.040.
[26] Y. Zhu, J. Liu, and X. Yang, "Design and performance analysis of a solar tracking system with a novel single-axis tracking structure to maximize energy collection," *Applied Energy*, vol. 264, 2020, doi: 10.1016/j.apenergy.2020.114647.
[27] F. Oliveira, G. Cruz, M. Barbosa, F. Junior, R. Lima, and L. Gómez-Malagón, "A proposal for a solar position sensor system with multifibre optical cable," *Sensors*, vol. 24, no. 11, 2024, doi: 10.3390/s24113269.

BIOGRAPHIES OF AUTHORS



Tran Duc Chuyen received his Doctor of Philosophy degree in industrial automation from Le Quy Don Technical University, Hanoi, Vietnam, in 2016. He was appointed an associate professor in 2024. He currently works at the Faculty of Electrical and Automation Engineering, University of Economics and Technology for Industries, Vietnam, where he also serves as chair of the faculty's scientific council. His research interests include electric machine design, electrical machines, drive systems, automatic control theory, power electronics and their applications, adaptive control, neural network control, robotic control, motion control, microcontrollers, the Internet of Things, intelligent control, and artificial intelligence. He can be contacted at email: tdchuyen@uneti.edu.vn.



Doan Van Vu graduated from university in 2024 and is currently pursuing a master's degree in electrical engineering at the University of Economics and Technology for Industries, Vietnam. He is also employed by Quat Group in Nam Dinh, Vietnam. His research interests include industrial electrical engineering, power supply systems, electrical installations, the Internet of Things, new and renewable energy, adaptive control, sliding-mode control, artificial neural network-based control, intelligent control, and artificial intelligence. He can be contacted at email: dvvu.24185200006@sv.uneti.edu.vn.